European Journal of Medicinal Chemistry 79 (2014) 77–88

Contents lists available at ScienceDirect

European Journal of Medicinal Chemistry

journal homepage: http://www.elsevier.com/locate/ejmech

Original article

Development of fluorescent double-strand probes labeled with 8-(*p*-CF_3-cinnamyl)-adenosine for the detection of cyclin D1 breast cancer marker

Lital Zilbershtein-Shklanovsky [a], Pinhas Kafri [b], Yaron Shav-Tal [b], Eylon Yavin [c], Bilha Fischer [a,*]

[a] Department of Chemistry, Gonda-Goldschmied Medical Research Center, Bar-Ilan University, Ramat-Gan 52900, Israel
[b] Faculty of Life Sciences and Institute of Nanotechnology, Bar-Ilan University, Ramat-Gan 52900, Israel
[c] School of Pharmacy, Institute for Drug Research, The Hebrew University of Jerusalem, Ein-Kerem, Jerusalem 91120, Israel

ARTICLE INFO

Article history:
Received 5 February 2014
Received in revised form
24 March 2014
Accepted 29 March 2014
Available online 30 March 2014

Keywords:
Oligonucleotide
Fluorescence
Hybridization
Cyclin D1 mRNA
Diagnostics

ABSTRACT

Fluorescent nucleoside analogs replacing natural DNA bases in an oligonucleotide have been widely used for the detection of genetic material. Previously, we have described 2-((4-(trifluoromethyl) phenyl)-*trans*-vinyl)-2′-deoxy-adenosine, **6**, a nucleoside analog with intrinsic fluorescence (NIF). Analog **6** exhibits a quantum yield 3115-fold higher than that of adenosine (φ 0.81) and maximum emission which is 120 nm red shifted (λ_{em} 439 nm). Here, we incorporated this analog in one or several positions of cyclin D1-targeting 15-mer oligonucleotides (ONs). The fluorescence of **6** was quenched upon incorporation into an oligonucleotide (ca. 1.5–22 fold), and was further reduced upon duplex formation. Specifically, **ON7** exhibited a fluorescence decrease of ca. 2- or 3-fold upon duplex formation with complementary DNA or RNA strand, respectively. We determined the kinetics of dehybridization/rehybridization process in the presence of ssDNA or ssRNA targets to optimize our probes length and established the probes' selectivity towards a specific target. Furthermore, we proved specificity of our probe to the target vs. singly mismatched targets. Our most promising *ds-NIF-probe*, **ON7**:RNA, was used for the detection of cyclin D1 mRNA marker in cancerous cells total RNA extracts. The ds-probe specifically recognized the target as observed by a 2-fold fluorescence increase within 30 s at RT. These findings illustrate the potential of *ds-NIF-probes* for the diagnosis of breast cancer.

1. Introduction

During the past decade, there has been a remarkable growth in the use of synthetic oligonucleotide probes in nucleic acid research for the detection of specific DNA or RNA sequences [1–3]. The sensitivity of fluorescence detection and its simplicity makes it an important tool in many areas and is being used for diagnostics of genetic and infectious diseases, discovery of gene-targeted drugs, molecular biology, and other biomedicinal studies [4,5].

Fluorescent nucleoside analogs with intrinsic fluorescence, based on the elongation of the natural purine/pyrimidine π-system replacing natural DNA bases in an oligonucleotide, have been developed by us and others as probes for detection of genetic material [6–12].

New fluorescent nucleoside probes have to meet the following requirements: they should be structurally similar to native nucleobases and capable of Watson–Crick pairing, their absorption and emission spectra should be red-shifted relative to those of native nucleosides, and they should exhibit 1000s-times higher quantum yields vs. natural nucleosides. Moreover, to become an effective tool for hybridization analysis, the labeled oligonucleotide has to display a considerable change of fluorescence upon hybridization with the complementary strand.

Purine nucleosides with intrinsic fluorescence include, for instance, 2-aminopurine (2AP), **1**, Fig. 1, (λ_{abs} 303 nm, λ_{em} 370 nm, φ 0.68 in neutral aqueous solution) [13,14]. The fluorescence of 2AP is strongly quenched within DNA, and this quenching is sensitive to

Abbreviations: A, adenosine; G, guanosine; C, cytosine; T, thymidine; ON, oligonucleotide; NIF, nucleoside with intrinsic fluorescence; TPPTS, tris(3-sulfonatophenyl) phosphine trisodium salt; MALDI, matrix-assisted laser desorption/ionization; BLAST, basic local alignment search tool; OD, optical density; PBS, phosphate buffer saline.

* Corresponding author.
E-mail address: bilha.fischer@biu.ac.il (B. Fischer).

http://dx.doi.org/10.1016/j.ejmech.2014.03.081
0223-5234/

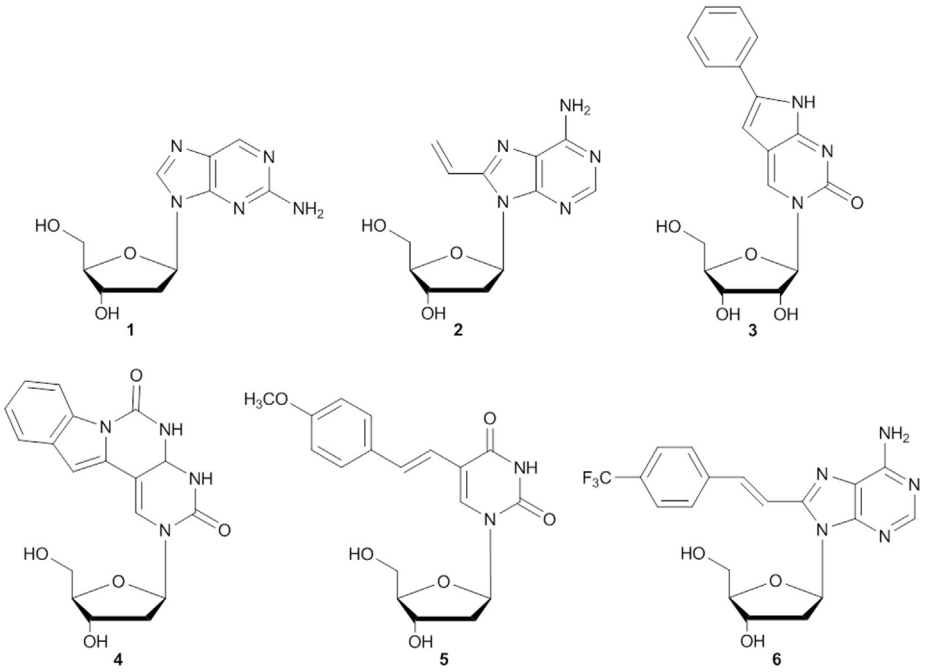

Fig. 1. Previously reported fluorescent purine and pyrimidine nucleoside analogs.

local and global changes in DNA conformation. Therefore this fluorophore has been employed to probe the structural and dynamic changes that characterize folding of ribozymes [15], DNA containing damage or mismatches [16,17], etc. Another known purine nucleoside probe is 8-vinyl-deoxyadenosine (8VdA), **2**, (λ_{abs} 290 nm, λ_{em} 388 nm, φ 0.66 in neutral aqueous solution) [18–20]. 8VdA exhibits similar base-pairing and base-stacking properties to those of adenine when introduced into double-stranded DNA (dsDNA). Moreover, the fluorescence quantum yield of 8VdA is sensitive to base stacking, making it a useful real-time probe of DNA structure [18]. However, both 2AP and 8VdA emit at relatively short wavelengths.

Pyrimidine nucleosides with intrinsic fluorescence include, for instance, 6-phenyl-pyrrolocytidine (^{Ph}pC), **3**, (λ_{abs} 360, λ_{em} 465 nm, φ 0.31 in phosphate buffer) [21,22]; pyrimidindole cytosine (dC^{PPI}), **4**, (λ_{max} 374, λ_{em} 513 nm, φ 0.006 in phosphate buffer) [23,24] and 5-((4-methoxy-phenyl)-*trans*-vinyl)-2′-deoxy-uridine, **5** (λ_{abs} 320 nm, λ_{em} 478 nm, φ 0.12 in H_2O) [8].

Recently, we reported on the promising properties of a novel adenosine analog with intrinsic fluorescence (nucleoside with intrinsic fluorescence, NIF), 2-((4-(trifluoromethyl) phenyl)-*trans*-vinyl)-2′-deoxy-adenosine, **6**, (λ_{abs} 340 nm, λ_{em} 439 nm, φ 0.81 in MeOH) [12]. This fluorescent adenosine analog bears a minimal chemical modification, at a position not involved in base-pairing, resulting in relatively long absorption and emission wavelengths and high quantum yield. Analog **6** exhibits a quantum yield that is 3115-fold higher than that of adenosine and maximum emission which is 120 nm red shifted. In addition, since analog **6** adopts an *anti* conformation and *S* sugar puckering, favored by B-DNA, it makes a promising nucleoside analog to be incorporated in an oligonucleotide probe for the detection of genetic material by a hybridization assay.

Here, we report on labeling cyclin D1-targeting 15-mer oligonucleotides by one or several monomer(s) of **6**, to be used as *ss-NIF-probes* or as *ds-NIF-probes*. Next, we determined the competency of monomer **6** to create Watson–Crick H-bond pairing in the same manner as adenosine by testing the probe vs. singly mismatched targets. We analyzed the dependence of photophysical properties and thermal stability of labeled ds-ONs on the number of labels, and on the neighboring nucleobases. Furthermore, we determined the kinetics of dehybridization/rehybridization process of *ds-NIF-probes* of different lengths with ssDNA or ssRNA targets, and also established the probes' selectivity towards a specific target. Finally, we demonstrated the use of the optimal *ds-NIF-probe*, **ON7**:RNA, for the detection of cyclin D1, a breast cancer mRNA marker, in total RNA extracts from cancerous cells.

2. Results

2.1. Design of NIF-labeled-oligonucleotide probes

We prepared 15-mer long ONs targeting cyclin D1 mRNA. Cyclin D1 protein is a major player in the control of the cell cycle [25]. The cyclin D1 gene has been convincingly implicated in oncogenesis, and it is highly expressed in many cancer types and has been specifically implicated in breast cancer [26]. From the original mRNA sequence of cyclin D1 consisting of 4304 nucleic acids, we selected a 15-mer sequence containing several T and A residues. We chose a 15-mer long oligonucleotide since this is the minimal length that would ensure specific binding to target cyclin D1. The specificity of the sequence was assessed by BLAST (basic local alignment search tool) [27].

Monomer **6** was used for the preparation of cyclin D1-targeting 15-mer ONs containing a single label or multi-labels replacing A at different positions of the oligonucleotide sequence. Since spectral properties of fluorescent nucleosides within ONs are sensitive to neighboring nucleobases [28–30], we incorporated monomer **6** at various positions of the studied 15-mer oligonucleotides. In addition, differently multi-labeled ONs were prepared to examine the influence of more than one label on fluorescence of the single-strand and of the resulting duplex.

The synthesized oligonucleotides were based on a 2′-OMe-RNA scaffold. 2′-OMe-RNA oligonucleotides are not substrates for RNaseH and show resistance to degradation by RNA- or DNA-specific nucleases [31]. In addition to being stable to standard handling and nuclease resistance, 2′-OMe-RNA oligomers form more stable hybrids with complementary RNA strands than equivalent DNA and RNA sequences [32,33].

Since fluorescence enhancement rather than quenching should be associated with a positive identification of a target, we propose two prototypes of NIF-labeled-oligonucleotide probes: a *ss-NIF-probe* and a *ds-NIF-probe*. Specifically, *ss-NIF-probe* is relatively dark, but, if it becomes fluorescent upon hybridization with a ssDNA or a ssRNA target, then ss-NIFs will be used as probes (Scheme 1).

However, if there is a decrease in the fluorescence intensity of the duplex as compared to ss-NIF-DNA fluorescence, a *ds-NIF-probe* will be used (Scheme 2). The *ds-NIF-probe*, **III**, (Scheme 2A) is relatively dark due to nucleobase interactions which result in quenching of fluorophore. Next, this ds-probe, **III**, is allowed to hybridize with a target sequence, **IV** (Scheme 2B). Here, we expect the formation of a new duplex, **V**, (Scheme 2B) and the release of fluorescent ss-NIF-DNA, **I**, thus indicating the presence of the target.

The requirements for application of this methodology for the detection of target DNA/RNA are that the free ss-NIF-DNA should be relatively fluorescent and NIF-DNA:DNA duplex should be relatively dark. Moreover, the ss-NIF-DNA should be shorter than its complementary oligonucleotide to faciliate dehybridization of **III** and re- hybridization with **IV**. If the target is mRNA the more stable DNA: mRNA duplex **V**, will be preferred over DNA–DNA duplex **III**. To apply the *NIF* methodology a considerable difference of fluorescence intensity (at least two fold) between the fluorescence of the free *ss-NIF-DNA* and that of the duplex NIF-DNA:DNA/RNA is required.

Two series of oligonucleotides were prepared to form the two prototypes of NIF-labeled-oligonucleotide probes. Specifically, the oligonucleotide was either complementary to the target mRNA (for the *ss-NIF-probe*) or identical to the target mRNA (for the *ds-NIF-probe*). These series of oligomers were used to explore whether our monomer of choice, **6**, when incorporated into a ss-oligonucleotide, would trigger a significant quantum yield change upon hybridization to a complementary sequence.

2.2. Incorporation of 8-(p-CF_3-cinnamyl)-2′-deoxy-adenosine (**6**) into oligonucleotides

To develop fluorescent oligonucleotide probes for the detection of DNA or RNA, we incorporated NIF-analog 8-(*p*-CF_3-cinnamyl)-2′-deoxy-adenosine, **6**, replacing 2′-deoxy-adenosine, into a single-strand oligonucleotide. We first prepared the protected and activated nucleoside phosphoramidite, **10**, starting from 8-Br-2′-deoxy-adenosine. [34] The latter was protected with 4, 4′-dimethoxytrityl group at C5′-OH, to obtain **7** in 73% yield, which was then employed as a substrate in a Suzuki coupling reaction with *trans*-2-[4-(trifluoromethyl)phenyl]vinylboronic acid to give **8** in 80% yield. Compound **8** was protected at the exocyclic N^6 with N,N-*dimethylformamide* dimethyl *acetal* to give **9** in 99% yield. Finally, the protected and activated nucleoside phosphoramidite, **10**, was obtained in 82% yield upon treatment of **10** with phosphoramidite chloride (Scheme 3).

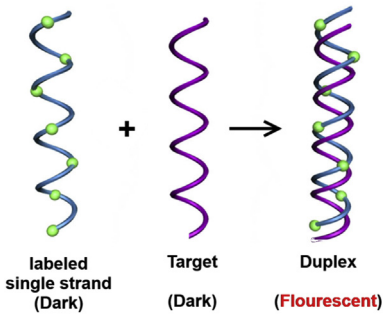

Scheme 1. A schematic illustration of the *ss-NIF-probe* methodology.

The modified ONs, containing analog **6**, were synthesized by standard solid-phase oligonucleotide synthesis and purified by reverse-phase HPLC. MALDI-TOF mass spectroscopy confirmed their identity.

2.3. Photophysical characterization of cyclin D1-targeting ss–NIF–probes

To identify an optimal *ss-NIF-probe*, five variously labeled single strand oligonucleotides were synthesized (**ONs 1**–**5**). Four of these oligonucleotides were mono-labeled with monomer **6** (**ONs 1**–**4**), at position 3 or 8 or 13 or 14, and one oligonucleotide was di-labeled at positions 3 and 8 (**ON5**), Scheme 4. For each oligomer the corresponding duplex was prepared. We studied both DNA:DNA duplexes and DNA:RNA duplexes due to possible differences in the fluorescent properties upon hybridization of **ONs 1**–**5** with complementary DNA or RNA.

Excitation and emission spectra of both single strands of labeled ONs and the corresponding duplexes were measured in PBS buffer (pH 7.4) in duplicates on two days, and the determined quantum yields are the average values of those measurements.

All studied ONs, either single or double strands, were excited at 338–344 nm and emit at 436–443 nm (Table 1). The quantum yields of all mono-labeled oligonucleotides decreased by ca. 1.5–2.5-fold upon DNA:DNA duplex formation. This trend was also observed for the corresponding DNA:RNA duplexes, however in these cases the decrease was more significant ca. 4.5–10-fold (Table 1). The di-labeled oligonucleotide did not exhibit a significant change in quantum yield upon DNA:DNA duplex formation (0.1 vs. 0.098), however, the quantum yield was decreased by ca. 2.5-fold upon DNA:RNA duplex formation. Since the *ss-NIF* probe method requires an increase of the quantum yield of the duplex compared to the single strand, none of these oligonucleotides can be used as a probe for the detection of mRNA.

2.4. Photophysical characterization of cyclin D1-targeting ds-NIF-probes

In this series, six labeled single strands oligonucleotides were synthesized. For each oligomer the corresponding duplex was prepared. Since this method requires the dehybridization of the duplex probe followed by the rehybridization of the target with its complementary strand and the release of the fluorescent single-strand (Scheme 2), the complementary strand was longer than the labeled strand (35-mer vs. 15-mer, respectively), to allow eventually formation of a longer and more stable duplex with the target RNA (see below optimization of the length of the complementary strand).

To identify an optimal *ds-NIF-probe*, six variously labeled single strand oligonucleotides were synthesized (**ONs 6**–**11**). Three of these oligonucleotides were mono-labeled at position 4, 9 or 14 (**ONs 6**–**8**), two were di-labeled at positions 4 and 9 (**ON9**), and 4 and 14 (**ON10**), and one was tri-labeled at positions 4, 9 and 14 (**ON11**), Scheme 5.

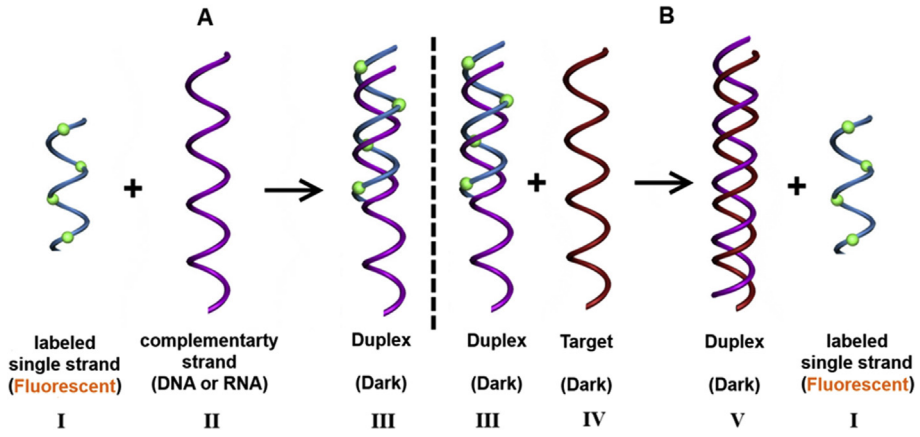

Scheme 2. A schematic illustration of the mechanism of action of a *ds-NIF-probe*. methodology.

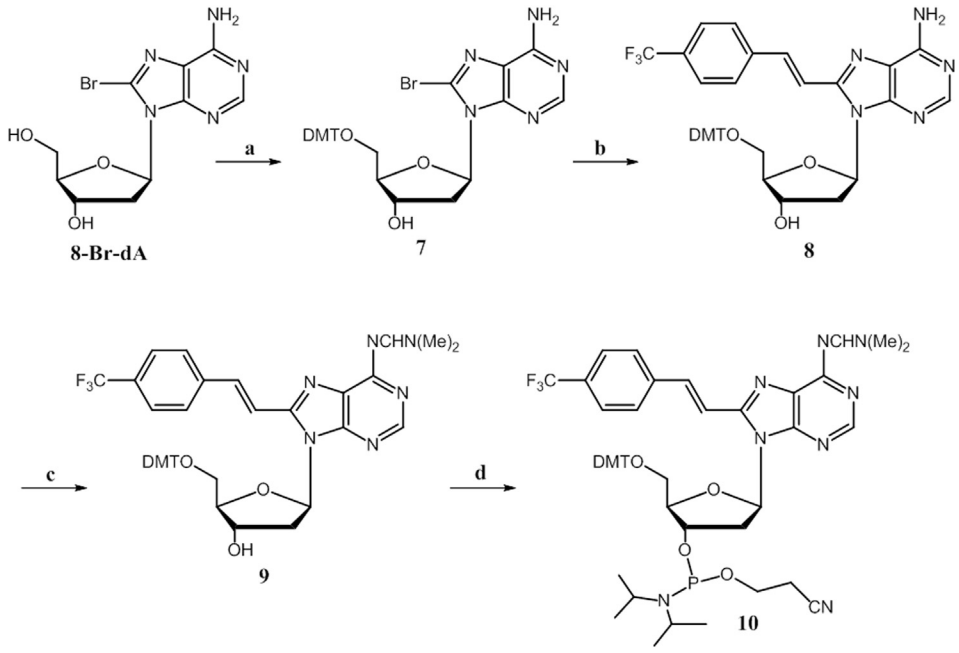

Scheme 3. Synthesis of phosphoramidite **10**. Reaction conditions: a) 4, 4′-dimethoxytrityl chloride (1.6 eq), TEA (2 eq), DMAP (0.25 eq), pyridine, 73% yield; b) trans-2-[4-(trifluoromethyl)phenyl]vinylboronic acid (1.25 eq), Na_2CO_3 (3 eq), TPPTS (0.25 eq), $Pd(OAC)_2$ (0.05 eq), CH_3CN:H_2O (1:2), 80% yield; c) N,N-*Dimethylformamide* dimethyl *acetal (6.5* eq*), DMF, 99 % yield;* d) N,N-diisopropylcyanoethyl-phosphoramidite chloride (1.2 eq), DIPEA (2.5 eq), DCM, 82% yield.

Unmodified ON: 5'- CUA CGC UAC UGU AAC -3'
*__Complementary ON__: 5'- GUU ACA GUA GCG UAG -3'
ON1: 5'- CU**A** CGC UAC UGU AAC -3'
ON2: 5'- CUA CGC U**A**C UGU AAC -3'
ON3: 5'- CUA CGC UAC UGU **A**AC -3'
ON4: 5'- CUA CGC UAC UGU A**A**C -3'
ON5: 5'- CU**A** CGC U**A**C UGU AAC -3'

A denotes fluorescent adenosine label. All other bases are 2'-OMe RNA.
* The complementary oligonucleotide is either a DNA or a RNA strand.

Scheme 4. Labeled-ONs for the preparation of *ss-NIF-probes* for the detection of cyclin D1 mRNA.

All studied ONs, either single or double strands, were excited at 336–343 nm and emit at 437–442 nm (Table 2). The measurements were performed in duplicates on two days, and the quantum yield values are averaged. Here, as for the *ss-NIF-probe*, we examined the change in fluorescence of the single strand upon DNA:DNA and DNA:RNA duplex formation.

Oligonucleotides mono-labeled at position 4 or 14 (**ONs 6** and **8**) did not exhibit a significant decrease of fluorescence upon duplex formation of the corresponding NIF-DNA:DNA or NIF-DNA:RNA (1.5, 1.2-fold or 1.8, 1.3-fold, respectively), Table 2. However, oligonucleotide mono-labeled at position 9 (**ON7**) displayed quantum yield value of 0.039, and this value was decreased by ca. 2-fold upon NIF-DNA:DNA duplex formation and by ca. 3-fold upon NIF-DNA:RNA duplex formation. The di-labeled oligonucleotides (**ONs 9** and **10**) exhibited a slight increase in quantum yields upon duplex formation, either NIF-DNA:DNA or NIF-DNA:RNA, while the quantum yield of the tri-labeled oligonucleotide (**ON11**) remained

Table 1
Photophysical properties of labeled cyclin D1-targeting ONs (**1**–**5**) designed as *ss-NIF* probes and their corresponding duplexes.[a]

	λ_{abs} max (nm)			λ_{em} max (nm)			φ		
	Single strand (ss)	Duplex with DNA	Duplex with RNA	Single strand (ss)	Duplex with DNA	Duplex with RNA	Single strand (ss)	Duplex with DNA	Duplex with RNA
ON1	343	339	340	437	440	438	0.14	0.056	0.033
ON2	340	340	340	436	436	440	0.25	0.176	0.044
ON3	341	342	340	440	436	440	0.37	0.29	0.084
ON4	340	344	340	443	443	439	0.55	0.37	0.055
ON5	342	338	343	439	441	443	0.1	0.098	0.04

[a] All measurements were carried out at 2 μM in a PBS buffer (pH 7.4) at room temperature.

unchanged upon NIF-DNA:DNA duplex formation, but exhibited a ca. 1.5-fold increase in quantum yield upon NIF-DNA:RNA duplex formation (Table 2).

2.5. Evaluating the ability of monomer **6** to retain the hybridization preference of adenosine

Analog **6** was designed to be incorporated into an oligonucleotide that upon hybridization will exhibit different fluorescence characteristics than the single-strand. Furthermore, monomer **6** should be capable of Watson–Crick base-pairing similarly to adenosine. For this purpose, **ON7** was hybridized to its perfectly matched complementary ON, and to singly mismatched ONs (Fig. 2).

Upon hybridization of **ON7** with its perfectly matched complementary ON, the fluorescence was quenched by ca. 3.5-fold. However, when the labeled **ON7** is hybridized with mismatched A/C/G ONs, the fluorescence was quenched only by ca. 2-fold, Fig. 3. Since similar results were obtained for all three mismatched ONs, we concluded that monomer **6** specifically recognizes T as an adenosine base does.

2.6. Reaction kinetics with double-stranded probes and a ssDNA target

Subsequent to proving the selectivity of 15-mer NIF probe **ON7**, we set to optimize the length of the complementary strand aiming at a facile dehybridization of the ds-NIF-probe followed by rehybridization with target mRNA.

For this purpose, we prepared a series of double-stranded ONs composed of **ON7** (15-mer) and complementary strands of different lengths (15- to 35-mer). The ds-probes were tested for their hybridization kinetics with a target single strand at room temperature. Specifically, instead of using the full mRNA of cyclin-D1, we used a 35-mer complementary DNA sequence. Fig. 4 shows the kinetic curves of the ds-NIF-probes hybridized to the 35-mer DNA target.

When the two strands were of equal length (Fig. 4A), or, when the complementary ON was a 17-mer oligonucleotide (Fig. 4B), no increase of fluorescence was observed over time, meaning no dehybridization/rehybridization process occurred. However, as the length difference of the complementary ONs increased, the reaction rate became faster (Fig. 4C–F). Specifically, when the overall difference between the strands was 5 nucleotides (nt) (Fig. 4C), the reaction still was not completed after 35 min. However, when the difference was 10 or 12 nt (Fig. 4D–E), maximum reaction was reached after 12 and 3 min, respectively. When the length difference exceeded 15 nt, maximum fluorescence was obtained after only 15 s (Fig. 4F–G).

Moreover, we have added a random 35-mer DNA to the *ds-NIF-probe* composed of (15-mer) **ON7**:DNA (35-mer) (Fig. 4H). Since no change in fluorescence intensity was observed in this case, we concluded that the dehybridization of the ds-probe (Fig. 4C–G) occurred due to specific target recognition and not due to spontaneous opening of the probe in the presence of any ON.

2.7. Reaction kinetics with double-stranded probes and a ssRNA target

The ds-probes mentioned above were made up of two complementary ONs at different length, when only at 5 nt difference a detectable hybridization/dehybridization process occurred. However, for RNA detection the two complementary ONs can be at the same length, or at least with a smaller nt difference between the two strands, since RNA forms a more stable duplex than DNA with a complementary strand. Since our ultimate goal was using these probes for the detection of mRNA, we tested the ds-NIF-probes for their hybridization kinetics with a target 30-mer ssRNA at room temperature. Fig. 7 shows the kinetic curves of the ds-probes hybridized with the target.

As shown in Fig. 5, when the two strands of the probe were of equal length (Fig. 5A), or, when the complementary ON was 17-mer (Fig. 5B), a small increase in fluorescence was observed, implying that dehybridization/rehybridization process has occurred (unlike for a DNA target). However, the reaction was very slow and after 35 min the reaction reached only 1/5 of the maximum fluorescence intensity. At 5 nt difference (Fig. 5C), after 35 min the reaction still did not reach its maximum. However, when the difference was 10 nt (Fig. 5D), maximum reaction occurred after 5 min. When the length difference exceeded 12 nt, maximum fluorescence was obtained after only 15 s (Fig. 5E–F).

In addition, we tested ds-NIF-probe containing equally long strands (15-mer each) with a 15-mer RNA target in which only 5 nt were complementary to the tested probe (Fig. 5G). However, when the ds-NIF-probe was added to this target RNA no reaction was observed.

2.8. Using ***ON7*** for the application of ds-NIF-probe methodology

To prove the applicability of analog **6** labeled ONs for detection of target ssDNA or ssRNA, we selected an ON exhibiting relatively significant change of fluorescence upon hybridization/dehybridization. Specifically, we selected a cyclin D1-targeting ON labeled at position 9 (**ON7**), the fluorescence of which is reduced ca. 2-fold upon NIF-DNA:DNA duplex formation and ca. 3-fold upon NIF-DNA:RNA duplex formation (Fig. 6).

2.9. Application of ds-NIF-probe for detection of cyclin D1 mRNA in total RNA extracts of cancerous cells

Next, to prove the applicability of the *ds-NIF* methodology for identification of a specific mRNA, we monitored the fluorescence intensity of the probe in total RNA extracted from the human U2OS osteosarcoma cell line. The selected *ds-NIF-probe* consisted of **ON7**

Unmodified ON: 5'- GUU ACA GUA GCG UAG -3'

***Complementary ON**: 5'- CACGGGCACGCUACGCUACUGUAACCAAGAGGGUA -3'

ON6: 5'- GUU **A**CA GUA GCG UAG -3'

ON7: 5'- GUU ACA GU**A** GCG UAG -3'

ON8: 5'- GUU ACA GUA GCG U**A**G -3'

ON9: 5'- GUU **A**CA GU**A** GCG UAG -3'

ON10: 5'- GUU **A**CA GUA GCG U**A**G -3'

ON11: 5'- GUU **A**CA GU**A** GCG U**A**G -3'

A denotes fluorescent adenosine label. All other bases are 2'-OMe RNA.
* The complementary oligonucleotide is either a DNA or a RNA strand.

Scheme 5. Labeled-ONs for the preparation of *ds-NIF-probes* for the detection of cyclin D1 mRNA.

(15-mer) hybridized with a complementary 30-mer RNA, since this probe exhibited the most significant change in fluorescence upon hybridization, exhibiting 3-fold decrease of fluorescence. The *ds-NIF-probe* (**ON7**:RNA) was added to total cell RNA extracts at a final concentration of 1 μM. The first extract was obtained from a cell line stably overexpressing the cyclin D1 gene, therefore containing high levels of cyclin D1 mRNA (up to 3-fold, as measured by quantitative RT-PCR, see Experimental section), while the second cell extract contained basal levels of cyclin D1 mRNA found in U2OS cells. Fluorescent **ON7** was used as a positive control, while ds-**ON7**:RNA probe was the negative control, and the fluorescence of RNA extract alone was tested as well.

Upon addition of ds-**ON7**:RNA probe to RNA extract containing high levels of cyclin D1, we observed an immediate increase in the fluorescent intensity up to 2-fold increase after only 30 s, relative to the negative control, indicating the release of the fluorescent 15-mer **ON7** and the formation of a RNA:cyclin D1 RNA duplex (Fig. 7).

Yet, addition of ds-**ON7**:RNA probe to total RNA extract of cells expressing basal levels of cyclin D1 did not result in any increase of fluorescence intensity (Fig. 8).

2.10. Thermostability of duplexes

The application of the above ONs, or corresponding duplexes, for the detection of genetic material depends on the thermostability of the related duplexes. The T_m values of the *ds-NIF-probe* should not be not too high to allow dehybridization before rehybridization with the target DNA/RNA (Scheme 2).

The T_m values of all hybrids fluorescent **ONs 1**–**11** with the complementary DNA or RNA strands are 48–66 °C, indicating that they are thermally stable (Table 3).

In most cyclin D1-targeting labeled duplexes T_m increased by 4–10 °C as compared to the unmodified duplex, for the DNA and for the RNA duplexes (Table 3). Exception to this increase was **ON3** (mono-labeled at position 13) that upon hybridization with DNA formed a less stable duplex by 7 °C and upon hybridization with RNA formed a duplex with the same stability as the unmodified duplex ($T_m = 56$ °C). Another exception was **ON4** (mono-labeled at position 14) that upon hybridization with DNA formed a less stable duplex by 5 °C ($T_m = 50$ °C).

In general, there was no significant T_m difference (0–3 °C) between duplexes in which the complementary strand was DNA or RNA, neither in the modified nor in the unmodified duplexes.

3. Discussion

We described the design and synthesis of NIF-labeled-oligonucleotide probes based on the incorporation of the fluorescent adenosine analog, **6**. The oligonucleotides were designed to be used for the detection of cyclin D1 mRNA, a breast cancer marker. We selected a 15-mer sequence from the cyclin D1 mRNA sequence, which is specific to this mRNA only and does not appear in any other endogenous mRNA, as was determined by BLAST.

We examined the influence of the incorporation of monomer **6** into an ON on the fluorescence of the former. **ONs 1**–**11** displayed reduced quantum yields relative to that of the free monomer **6** (0.033–0.55 compared to 0.74). We observed that the fluorescence intensities (which correlate with quantum yield) of the ONs are not dependent on the location of the label in the ON, but, on the neighboring nucleobases. In particular, ONs in which at least one of the neighboring nucleobases of the labeled monomer was guanine exhibited the lowest quantum yields (e.g., **ONs 7**–**11**). On the contrary, ONs in which at least one of the neighboring nucleobases of the labeled residue was adenine, exhibited the highest quantum yields, as long as the other neighbor was not guanine (e.g., **ONs 3** and **4**). The highest quantum yield was obtained for **ON4** with adenine and cytidine neighbors. In general, ONs in which the label had thymidine and cytidine as neighbors exhibited high quantum yields, $\varphi \geq 0.1$ (e.g., **ONs 1**, **2**, **5** and **6**). No additive effect was observed for multi-labeled ON. Moreover, di/tri-labeled ONs exhibited an average quantum yield typical of mono-labeled ONs (e.g., **ON10** vs. **ONs 6** and **8**, φ 0.072, 0.296 and 0.037, respectively).

Development of a hybridization-based fluorescent probe requires not only different photophysical properties in labeled single strand vs. labeled duplex, but also duplex stability. If the labeled duplex probe is unstable, namely, T_m value of the labeled duplex is too low, it is of no use. Thus, we studied the dependence of the thermo-stability of the labeled-duplexes on the site of the label and number of labels. Surprisingly, we found that incorporation of monomer **6** in ONs increases the stability of the resulting duplexes, and in most labeled duplexes, T_m increased by 4–10 °C as compared to the unmodified duplex.

Moreover, no significant change was observed for mono-, di-, or tri-labeled duplexes in terms of stability. For instance, **ONs 1**, **2**, and **5** (mono-labeled at positions 3 or 8, or di-labeled at positions 3 and 8, respectively) exhibited almost the same T_m value (T_m = 59–60 °C) for the DNA and for the RNA duplexes. The increased stability of these duplexes may indicate favorable stacking interactions of monomer **6**, as compared to those of A itself with its neighboring nucleobases.

We synthesized two prototypes of probes: *ss-NIF-probes* and *ds-NIF-probes*. However, since a decrease of fluorescence was obtained upon duplex formation in both cases, only the *ds-NIF-probe* methodology was further pursued. For testing our methodology we used our most promising probes-**ON7**:DNA and **ON7**:RNA, which exhibited the most significant change in fluorescence upon duplex formation (2- and 3-fold, respectively).

We first proved that monomer **6** exhibits the same base-pairing pattern as adenosine, and therefore shows the same hybridization preference. Monomer **6** labeled **ON7** was hybridized with four ONs: a perfectly matched complementary ON, and three singly mismatched ONs. **ON7** exhibited larger fluorescence quenching upon hybridization to its perfectly matched complementary ON, as compared to hybridization to the singly mismatched ONs (3.5-fold vs. 2-fold), indicating that monomer **6** and adenosine recognize T in the same manner.

Next, we optimized the length of our *ds-NIF-probe* (**ON7**:DNA) by studying the reaction kinetic of duplexes having complementary strands of different lengths upon addition of cyclin D1-based ssDNA or ssRNA targets, at room temperature. Moreover, the targets were either perfectly matched to the studied probes or random DNA targets to evaluate the probes' selectivity towards a specific target sequence.

Table 2
Photophysical properties of labeled cyclin D1-targeting ONs (**6-11**) designed as *ds-NIF* probes and their corresponding duplexes.[a]

	λ_{abs} max (nm)			λ_{em} max (nm)			φ		
	Single strand (ss)	Duplex with DNA	Duplex with RNA	Single strand (ss)	Duplex with DNA	Duplex with RNA	Single strand (ss)	Duplex with DNA	Duplex with RNA
ON6	340	343	342	441	440	441	0.296	0.197	0.164
ON7	337	343	343	439	440	440	0.039	0.021	0.014
ON8	336	336	339	437	437	439	0.037	0.032	0.029
ON9	339	343	341	441	439	439	0.042	0.062	0.067
ON10	342	343	343	439	441	441	0.072	0.079	0.086
ON11	340	342	342	440	442	439	0.033	0.031	0.046

[a] All measurements were carried out at 2 μM in a PBS buffer (pH 7.4) at room temperature.

ON7: 5'- GTT ACA GT**A** GCG TAG -3'
match: 3'- CAA TGT CA**T** CGC ATC -5'
mismatch-A: 3'- CAA TGT CA**A** CGC ATC -5'
mismatch-C: 3'- CAA TGT CA**C** CGC ATC -5'
mismatch-G: 3'- CAA TGT CA**G** CGC ATC -5'

Fig. 2. The sequences of matched and mismatched ONs for hybridization with **ON7**.

For the DNA targets, even though a detectable reaction between the ds-NIF-probe and the target was observed at 5 nt difference (Fig. 6C), only when the difference was ≥10 nt, the reaction reached its maximum within 12 min (Fig. 6D). The optimal probes reacting immediately, in less than 15 s, were obtained for ds-NIF-DNA:DNA in which the difference was ≥15 nt (Fig. 6F).

However, when using the latter probes for the detection of a RNA target (Fig. 7), even though a detectable reaction was observed when the two strands of the probe were of equal length, only when the difference was ≥10 nt, the reaction reached its maximum within 5 min (Fig. 7D). An immediate reaction (less than 15 s) was achieved when the difference between the lengths of the strands in the ds-NIF-probe was ≥12 nt (Fig. 7E–F).

These probes were designed to be used for the detection of mRNA. Therefore, after proving their ability to detect selectively ssDNA and ssRNA sequences representing part of target mRNA, we demonstrated the ability of the optimal *ds-NIF-probe* **ON7**:RNA to detect selectively cyclin D1 mRNA in total RNA extracts from cancerous U2OS cells. An immediate increase in fluorescence up to 2-fold was observed following the addition of the probe to the extract containing high levels of cyclin D1 vs. extract containing basal levels cyclin D1, indicating the recognition of the target mRNA by the probe.

To conclude, we propose a novel probe for the efficient and selective detection of cyclin D1 mRNA. This probe is based on the incorporation of the fluorescent monomer, **6**, into an oligonucleotide to create a fluorescent single-strand. When the latter labeled strand forms a duplex with a complementary unmodified strand, the fluorescence is quenched, resulting in a relatively dark duplex probe. Upon addition of a target single-strand to the dark probe a new and more stable duplex is formed with the release of the fluorescent oligonucleotide.

We validated our methodology by successfully detecting DNA and RNA variants of cyclin D1 as well as cyclin D1 mRNA from cell extracts using the relatively dark **ON7**:RNA duplex probe. These results support the potential usefulness of **ON7**:RNA probe for the diagnosis of breast cancer.

A significant advantage of our new methodology is that the ON itself is intrinsically fluorescent and there is no need for additional experimental procedures for the attachment of a fluorophore prior to detection.

Our findings are a stepping stone to a further design of new and more efficient probes based on NIF-method.

4. Experimental

4.1. General

Compounds were characterized by NMR using a Bruker AC-200, DPX-300 or DMX-600 spectrometers. Chemical shifts are expressed in ppm downfield from Me_4Si (TMS), used as internal standard. The values are given in δ scale. All air and moisture sensitive reactions were carried out in flame-dried, nitrogen flushed flasks sealed with rubber septa, and the reagents were introduced with a syringe. All reactants in moisture sensitive reactions were dried overnight in a vacuum oven. Progress of the reactions was monitored by TLC on precoated Merck silica gel plates (60F-254). Visualization was accomplished by UV light. Flash chromatography was carried out on silica gel (Davisil Art. 1000101501). Medium pressure chromatography was carried out using automated flash purification system (Biotage SP1 separation system, Uppsala, Sweden). New compounds were analyzed under ESI (electron spray ionization) conditions on a Q-TOF micro-instrument (Waters, UK) and high resolution MS-MALDI-TOF spectra were recorded with an autoflex TOF/TOF instrument (Bruker, Germany). Absorption spectra were measured on a UV instrument (UV–2401PC UV–VIS recording spectrophotometer, Shimadzu, Kyoto, Japan) using a 10 mm quartz cell with 1 cm path length. Emission spectra were measured using Aminco-Bowman series 2 (AB2) Luminescence Spectrometer (Thermo electron corporation, Markham, Ontario, Canada). Reaction kinetics of displacement hybridization experiments were measured using Cary Eclipse Fluorescence Spectrophotometer. Thermal denaturation curves measurements were performed on a Cary 300 UV–visible spectrophotometer (Varian Inc.). Absorption and fluorescence spectra were recorded in PBS buffer containing NaC1 8.0 g, KC1 0.2 g, Na_2HPO_4 1.15 g, KH_2PO_4 0.2 g, and water 100 mL (pH 7.4). The unmodified oligonucleotides were purchased from Integrated DNA Technologies (Coralville, Iowa, USA). Modified oligonucleotides were synthesized by standard automated solid-phase method on an AKTA oligopilot plus oligonucleotide synthesizer. All commercial reagents were used without further purification.

4.2. Extinction coefficients calculations

The following 260 nm extinction coefficients were used to determine the concentration of the modified oligonucleotides: $\varepsilon G = 11{,}500\ M^{-1}\ cm^{-1}$, $\varepsilon_A = 15{,}400\ M^{-1}\ cm^{-1}$, $\varepsilon_U = 9900\ M^{-1}\ cm^{-1}$, $\varepsilon_C = 7200\ M^{-1}\ cm^{-1}$ and ε (modified)$A = 17{,}640\ M^{-1}\ cm^{-1}$. The extinction coefficients of the duplexes (ε_D) are less than the sum of

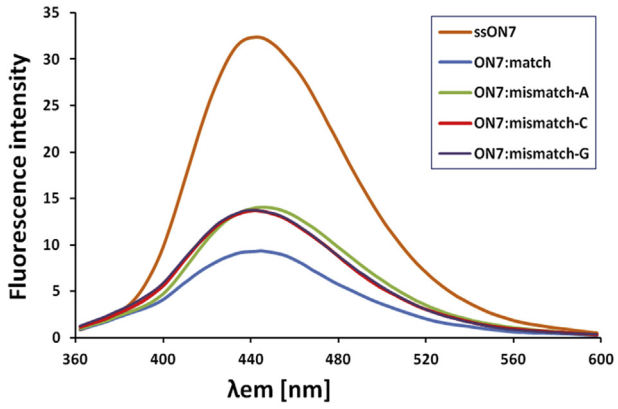

Fig. 3. Emission spectra of **ON7** alone and hybridized with the four targets (match; mismatch-A; mismatch-C; mismatch-G) after excitation at 340 nm. All duplexes and single strand were measured at 2 μM in a PBS buffer (pH 7.4) at room temperature.

where f_{AT} and f_{GC} are the fractions of the AT and GC base pairs, respectively.

4.3. Oligonucleotide synthesis and purification

The modified 2′-OMe oligonucleotides were synthesized at 3 μmol scale using a conventional automated solid-phase protocol using natural β-cyanoethylphophoramidite nucleosides. The coupling time of the modified base was increased from 2 to 10 min. Cleavage from the solid support and oligonucleotide deprotection was carried out in a 3.5 M solution of NH_3 in MeOH (300 μL) at RT for 2 h, followed by treatment with 33% NH_4OH (250 μL) at 55 °C for overnight. The residue was washed with EtOH:H_2O 1:1 (0.4 mL), and following spin down, the resulting aqueous solution was removed by speed-vac. Final purification of the oligonucleotides was achieved on a HPLC (Merck–Hitachi) system using a semi-preparative reverse phase column (Gemini 5u C-18 110A, 250 mm × 10 mm, 5 μm, Phenomenex, Torrance, CA, USA), in TEAA

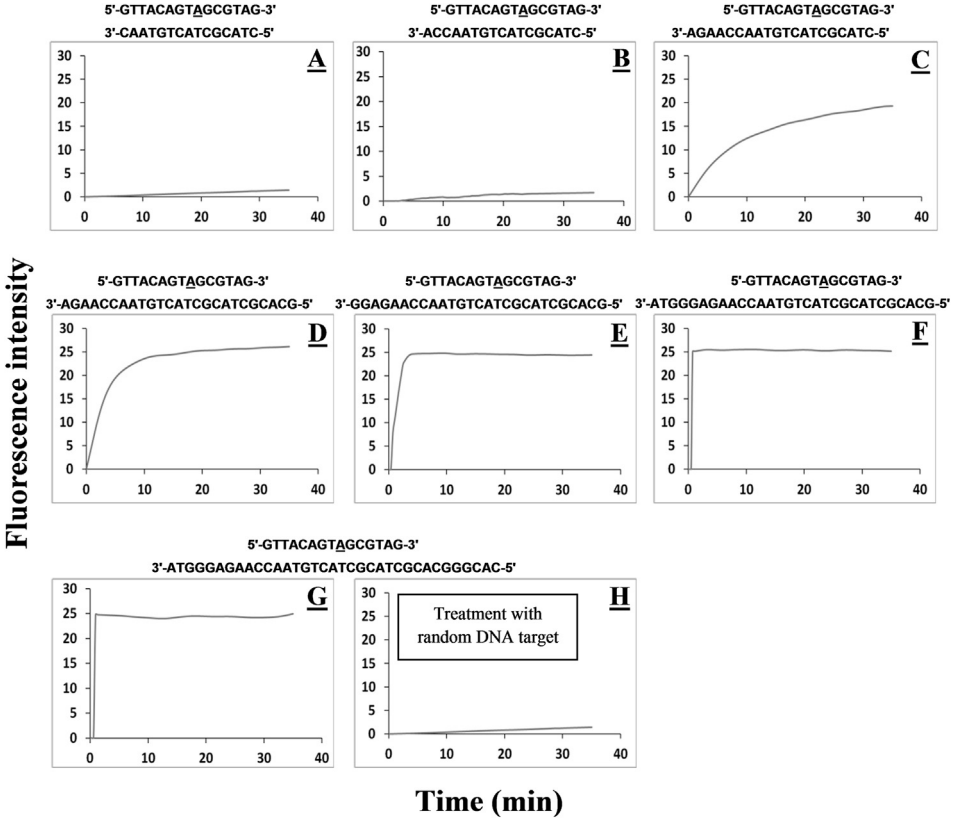

Fig. 4. Reaction kinetics of displacement hybridization between ds-ONs and a 35-mer DNA target. The final concentrations of the ds-ON probe and the target strand in the solution were 2 μM and 4 μM, respectively. The sequences of the ds-ONs tested are listed at the top of each graph, where underlining identifies the modified nucleoside substituent. In graphs **A**-**G** the listed ds-ONs were treated with a perfectly complementary target 5′-TACCCTCTTGGTTACAGTAGCGTAGCGTGCCCGTG-3′, and in graph **H** the listed ds-ON was treated with a random 35-mer DNA target 5′-CTATTCTCGCTACCGGAAGTATCGTGTCCGTGCGC-3′.

the extinction coefficients of their complementary strands (ε_{S1}, ε_{S2}), due to hypochromic effect that should be taken into account [35]. Therefore, the extinction coefficients were calculated by the following equation:

$$\varepsilon_D = (1 - h_{260\ nm})(\varepsilon_{S1} + \varepsilon_{S2})$$

$$h_{260\ nm} = 0.287 f_{AT} + 0.059 f_{GC}$$

buffer (0.1 M, pH 7.0): ACN 87:13 to 75:25 in 30 min at a flow rate of 5 mL/min. Purity was determined by analytical HPLC and confirmed >95% pure. All modified ONs were confirmed by MALDI-TOF mass spectrometry.

ON1 calcd for $C_{164}H_{210}F_3N_{53}O_{102}P_{14}$: 5045, found 5048.
ON2 calcd for $C_{164}H_{210}F_3N_{53}O_{102}P_{14}$: 5045, found 5047.
ON3 calcd for $C_{164}H_{210}F_3N_{53}O_{102}P_{14}$: 5045, found 5047.
ON4 calcd for $C_{164}H_{210}F_3N_{53}O_{102}P_{14}$: 5045, found 5045.

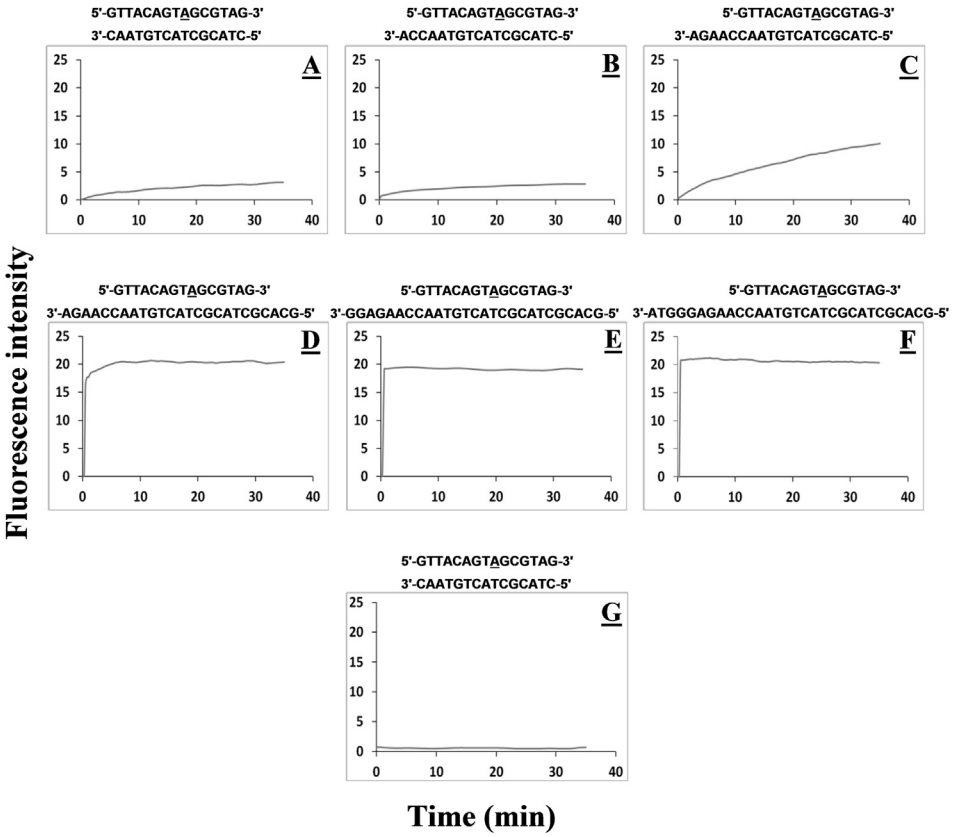

Fig. 5. Reaction kinetics of displacement hybridization between ds-ONs and a 30-mer RNA target. The final concentrations of the ds-ON probe and the target strand in the solution were 2 μM and 4 μM, respectively. The sequences of the ds-ONs tested are listed at the top of each graph, where underlining identifies the modified nucleoside substituent. In graphs **A**-**F** the listed ds-ONs were treated with a perfectly complementary target 5′-UACCCUCUUGGUUACAGUAGCGUAGCGUGC-3′, and in graph **G** the listed ds-ON was treated with RNA target contains only 5 complementary nt 5′-UACCG AGUAGAUCGU-3′.

ON5 calcd for $C_{172}H_{215}F_6N_{53}O_{101}P_{14}$: 5187, found 5187.
ON6 calcd for $C_{167}H_{210}F_3N_{59}O_{102}P_{14}$: 5165, found 5168.
ON7 calcd for $C_{167}H_{210}F_3N_{59}O_{102}P_{14}$: 5165, found 5163.
ON8 calcd for $C_{167}H_{210}F_3N_{59}O_{102}P_{14}Na$: 5188, found 5184.
ON9 calcd for $C_{175}H_{213}F_6N_{59}O_{101}P_{14}$: 5307, found 5311.
ON10 calcd for $C_{175}H_{213}F_6N_{59}O_{101}P_{14}$: 5307, found 5308.
ON11 calcd for $C_{183}H_{216}F_9N_{59}O_{100}P_{14}K$: 5484, found 5489.

4.4. UV measurements

The concentrations of all single-stranded and double-stranded oligonucleotides were 2 μM in PBS buffer (pH 7.4), and were determined by UV absorption measurement at 260 nm. Samples were measured at room temperature in a 10 mm quartz cell with a 1 cm path length.

4.5. Fluorescence measurements

Emission spectra of all the single-stranded and double-stranded oligonucleotides were measured in PBS buffer (pH 7.4) at the concentration of 2 μM. Measurements conditions included: excitation at 340 nm, 650 V sensitivity, and a 5 nm slit. Samples were measured at room temperature in a 70 μL quartz cell with path length of 1 cm.

4.6. Quantum yield determination

The quantum yields (φ) of the single-stranded and double-stranded oligonucleotides were calculated from the observed absorbance and the area of the fluorescence emission band. The fluorescence quantum yields of all oligonucleotides were determined relative to quinine sulfate in 0.1 M H_2SO_4 (λ_{ex} 350 nm, λ_{em} 446 nm, φ 0.54) [36]. The quantum yield was calculated according to the following equation:

$$\varphi = \varphi_R \frac{I}{I_R} \frac{OD_R}{OD} \frac{\eta^2}{\eta_R^2}$$

Here, φ and φ_R are the fluorescence quantum yield of the sample and the reference, respectively, I and I_R are areas under the fluorescence spectra of the sample and of the reference, respectively, OD and OD_R are the absorption values of the sample and the reference at the excitation wavelength, and η and η_R are the refractive index for the respective solvents used for the sample and the reference.

4.7. Hybridization of oligonucleotides

Solutions of labeled single-strands were mixed at room temperature with an equimolar amount of the complementary single strand oligonucleotides in PBS buffer (pH 7.4). Samples were hybridized by heating to 90 °C for 5 min and subsequently allowed to cool to room temperature over 2 h prior to measurements.

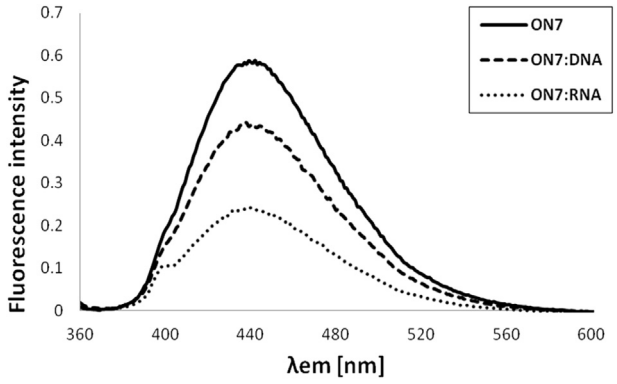

Fig. 6. Emission spectra of Cyclin D1-derived **ON7** vs. its duplexes with complementary DNA and RNA strands.

4.8. Thermal denaturation measurements (T_m)

The T_m values of duplexes were measured in PBS buffer (pH 7.4) at 1 μM concentrations. The absorbance of the samples was monitored at 260 nm and the temperature ranged from 20 to 85 °C with heating rate of 1 °C/min.

4.9. Reaction kinetics of displacement hybridization

The reaction kinetics experiments of double-stranded probes were carried out at room temperature in a 70 μL quartz fluorescence cell with path length of 1 cm. Fluorescence was measured upon excitation at 340 nm. The final concentration of the double-stranded probe and the target strand in the solution was 2 μM and 4 μM, respectively (to ensure full hybridization).

4.10. Cell culture and RNA cell extract

Human U2OS osteosarcoma cells were maintained in low glucose Dulbecco's Modified Eagle's Medium (DMEM, Biological Industries, Israel) containing 10% fetal bovine serum (FBS, HyClone, Logan, UT). The clone overexpressing cyclin D1 contained a stable integration of a GFP-cyclin D1 plasmid under the control of the CMV promoter. RNA was extracted from wild-type U2OS cells and cyclin D1 overexpressing cells using TRI Reagent Sigma–Aldrich protocol.

For RT-PCR, DNA-free Kit (Ambion) was used to remove genomic DNA contamination. cDNA (1 μg RNA) was synthesized using the ReverseAid First Strand cDNA Synthesis Kit (Fermentas) with oligo-dT as a primer. Semiquantitative RT-PCR was performed using Eppendorf Thermocycler amplification for 19–38 cycles (depending on the saturation level of the genes amplified) using 1 min denaturation at 94 °C, 1 min annealing at 55 °C for GAPDH and 62 °C for cyclin D1, 1 min extension at 72 °C, and 72 °C for 10 min for final extension. Primers for GAPDH: sense, ACC ACA GTC CAT GCC ATC AC; antisense, TCC ACC ACC CTG TTG CTG TA. Primers for cyclin D1: sense, ATA CTC GAG CCA TGG AAC ACC AGC TCC TGT GC; antisense, GCA ACG AAG GTC TGC GCG TGT TTG C.

Levels of cyclin D1 mRNA expression were three times higher in U2OS cells overexpressing GFP-cyclin D1 than in wild-type U2OS cells (WT), as measured by quantitative RT-PCR. Glyceraldehyde-3-phosphate dehydrogenase (GAPDH) mRNA levels were used as a control.

4.11. Fluorescence measurements of double-stranded probe in total cell RNA extracts

Fluorescence measurements of double-stranded probe, **ON7**:RNA, in RNA extracts were performed at room temperature in PBS buffer (pH 7.4). The final concentration of the probe was 1 μM, while the concentration of the total RNA extracts ranged from 6000 to 7500 ng/μL. The fluorescence was measured upon excitation at 340 nm. Samples were measured in a 10 mm quartz cell with a 1 cm path length. Duplicate samples were measured and the experiments were performed on two days using two different total RNA extract batches.

4.12. Synthesis

4.12.1. 5-(6-Amino-8-bromo-9H-purin-9-yl)-2-((bis(4-methoxyphenyl)(phenyl) methoxy)methyl)tetrahydrofuran-3-ol (**7**) [34]

8-Bromo-2′-deoxyadenosine (1 g, 3.03 mmol) was co-evaporated with dry pyridine and then dissolved in dry pyridine (15 mL). Et_3N (0.845 mL, 6.06 mmol), DMAP (93 mg, 0.7575 mmol), and DMT-Cl (1.64 g, 4.848 mmol) were added under N_2, and the mixture was stirred at RT. for 5 h. Then, MeOH (2.5 mL) was added and the mixture was extracted with DCM. The organic phase was washed with sat. $NaHCO_3$ soution, the combined organic layer was dried (Na_2SO_4) and concentrated, and the residue was purified on a silica gel column using DCM:MeOH, 98:2, as the eluant. Analog **50** was obtained as a light yellow foam (1.4 g, 73%). Mp 122 °C; ^{1}H NMR (600 MHz, DMSO-d_6): δ 7.99 (s, 1H), 7.39 (s, 2H), 7.26 (d, J = 7.5 Hz, 2H), 7.20–7.12 (m, 7H), 6.78 (d, J = 9 Hz, 2H), 6.75 (d, J = 9 Hz, 2H), 6.30 (m, 1H), 5.35 (d, J = 4.5 Hz, 1H), 4.71 (m, 1H), 3.95 (m, 1H), 3.72 (s, 3H), 3.71 (s, 3H), 3.48 (m, 1H), 3.17 (m, 1H), 3.07 (m, 1H) 2.27 (m, 1H) ppm; ^{13}C NMR (150 MHz, DMSO-d_6): δ 157.9, 157.9, 154.9, 152.4, 150.0, 144.9, 135.7, 135.6, 129.6, 129.5, 127.6, 127.2, 126.4, 119.5, 113.0, 112.9, 85.6, 85.5, 85.1, 70.4, 63.3, 55.0, 54.9, 48.6, 36.2 ppm. MS ES+ m/z: 655 (MNa^+); HR MALDI calcd for $C_{31}H_{30}BrN_5NaO_5$: 654.1323, found 654.1270.

4.12.2. 5-(6-Amino-8-(4-(trifluoromethyl)styryl)-9H-purin-9-yl)-2-((bis(4-methoxy-phenyl)(phenyl)methoxy)methyl) tetrahydrofuran-3-ol (**8**) [37,38]

Water–acetonitrile (2: 1, 15 mL) mixture was added through a septum to a nitrogen purged vial containing **7** (500 mg, 0.791 mmol, 1 eq), trans-2-(4-fluorophenyl)vinylboronic acid (214 mg, 0.989 mmol, 1.25 eq), $Pd(OAc)_2$ (11 mg, 0.04 mmol, 0.05 eq), Na_2CO_3 (252 mg, 2.373 mmol, 3 eq), and TPPTS (113 mg,

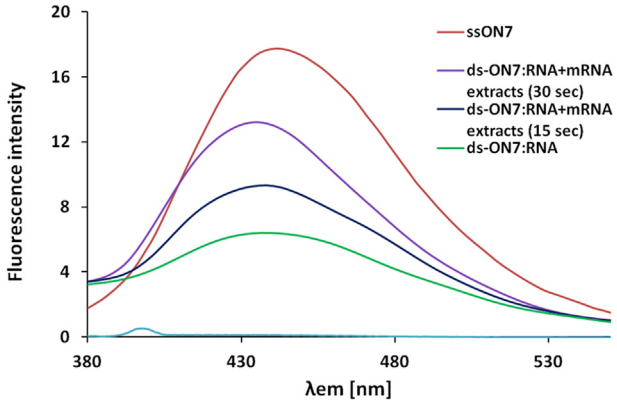

Fig. 7. Fluorescence spectra of ds-**ON7**:RNA probe in the presence of total RNA cell extract containing high levels of cyclin D1 mRNA.

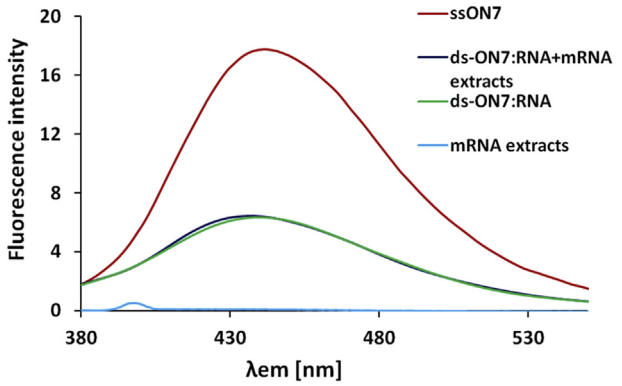

Fig. 8. Fluorescence spectra of ds-**ON7**:RNA probe in the presence of total RNA cell extract containing basal levels of cyclin D1 mRNA.

0.198 mmol, 0.25 eq). The mixture was stirred at 90 °C under N_2 atmosphere for 3 h until a brown-yellow residue was obtained. The reaction was cooled to room temperature and few drops of concentrated HCl were added (pH ~ 7). The product was purified on a silica gel column using $CHCl_3$:MeOH, 97:3, as the eluant, and was obtained as a yellow foam (458 mg, 80%). Mp 134 °C; ^{1}H NMR (300 MHz, DMSO-d_6): δ 8.07 (s, 1H), 7.94 (d, J = 8.4 Hz, 2H), 7.84 (d, J = 15.9 Hz, 1H), 7.75 (d, J = 8.4 Hz, 2H), 7.71 (d, J = 15.9 Hz, 1H), 7.30 (s, 2H), 7.21–7.08 (m, 9H), 6.70 (m, 5H), 5.36 (d, J = 5 Hz, 1H), 4.76 (m, 1H), 3.94 (m, 1H), 3.65 (s, 3H), 3.64 (s, 3H), 3.55 (m, 1H), 3.20 (m, 1H), 3.05 (m, 1H), 2.30 (m, 1H) ppm; ^{13}C NMR (150 MHz, DMSO-d_6): δ 157.8, 155.7, 152.3, 149.8, 147.7, 144.9, 139.7, 135.6, 135.5, 133.8, 129.5, 129.5, 129.0, 128.7, 128.4, 127.9, 127.6, 127.5, 126.4, 125.7, 125.7, 125.1, 123.3, 119.4, 117.8, 112.9, 112.9, 85.2, 85.0, 83.3, 79.1, 70.2, 63.1, 54.8, 37.1 ppm. MS ES+ *m/z*: 746 (MNa^+); HR MALDI calcd for $C_{40}H_{36}F_3N_5NaO_5$: 746.2561, found 746.2550.

*4.12.3. N′-(9-(5-((bis(4-methoxyphenyl)(phenyl)methoxy)methyl)-4-hydroxytetra-hydrofuran-2-yl)-8-(4-(trifluoromethyl)styryl)-9H-purin-6-yl)-N,N-dimethylformimidamide (**9**) [39]*

Dimethylformamidine acetal (0.63 mL, 4.72 mmol, 6.5 eq) was added to a solution of **64** (525 mg, 0.7262 mmol, 1 eq) in dry DMF (16 mL). The mixture was stirred for 24 h at 60 °C and the solvent was removed under vacuum to produce a light-yellow solid (565 mg, 99%). Mp 114 °C; ^{1}H NMR (300 MHz, DMSO-d_6): δ 8.93 (s, 1H), 8.32 (s, 1H), 8.01 (d, J = 8.4 Hz, 2H), 7.97 (d, J = 16.5 Hz, 1H), 7.77 (d, J = 8.4 Hz, 2H), 7.74 (d, J = 16.5 Hz, 1H), 7.19–7.05 (m, 9H), 6.68 (m, 5H), 5.39 (d, J = 5.1 Hz, 1H), 4.78 (m, 1H), 3.94 (m, 1H), 3.63 (s, 6H), 3.60–3.40 (m, 2H), 3.23 (s, 3H), 3.16 (s, 3H), 3.06 (m, 1H), 2.30 (m, 1H) ppm; ^{13}C NMR (150 MHz, DMSO-d_6): δ 158.6, 157.8, 157.8, 157.6, 151.9, 151.4, 149.4, 144.8, 139.7, 135.6, 134.8, 129.5, 129.4, 128.9, 128.6, 128.1, 127.6, 127.5, 126.4, 126.0, 125.6, 125.6, 125.1, 123.3, 117.5, 112.9, 112.9, 85.2, 85.0, 83.4, 70.2, 63.1, 54.8, 40.7, 37.2, 34.6 ppm. MS ES+ *m/z*: 779 (MH^+); HR MALDI calcd for $C_{43}H_{42}F_3N_6O_5$: 779.3163 found 779.3130.

Table 3
Thermal Denaturation Temperatures of cyclin D1-targeting ONs (**1**–**11**) measured at 1 μM in a PBS buffer (pH 7.4).

	T_m (°C)			T_m (°C)	
	Duplex with DNA	Duplex with RNA		Duplex with DNA	Duplex with RNA
Unmodified ON	55	56	**ON6**	64	65
ON1	59	60	**ON7**	61	60
ON2	60	60	**ON8**	64	61
ON3	48	56	**ON9**	64	62
ON4	50	65	**ON10**	65	64
ON5	60	60	**ON11**	65	66

*4.12.4. 2-((Bis(4-methoxyphenyl)(phenyl)methoxy)methyl)-5-(6-((Z)-(dimethylamino) methyleneamino)-8-(4-(trifluoromethyl) styryl)-9H-purin-9-yl)tetrahydrofuran-3-yl 2-cyanoethyl diisopropylphosphoramidite (**10**) [34]*

A solution of **9** (800 mg, 1.03 mmol, 1 eq) in dry DCM (9 mL) was treated with DIPEA (448 μL, 2.57 mmol, 2.5 eq) and 2-cyanoethyl diisopropyl-phosphoramidochloridite (276 μL, 1.23 mmol, 1.2 eq). After stirring for 22 h at RT, the product was purified on a silica gel column using hexane/AcOEt 90:10 - 40:60 (+3% Et_3N), as the eluant, and was obtained as a yellow powder (810 mg, 81%). Mp 78–79 °C; ^{1}H NMR (200 MHz, $CDCl_3$): δ 8.89 (s, 1H), 8.36 (s, 1H), 8.09 (d, J = 15.6 Hz, 1H), 7.65–7.33 (m, 7H), 7.22–7.12 (m, 6H), 6.65 (m, 5H), 6.54 (m, 1H), 4.93 (m, 1H), 4.26 (m, 1H), 3.71 (s, 6H), 3.70–3.46 (m, 7H), 3.30 (s, 3H), 3.22 (s, 3H), 2.76–2.44 (m, 3H), 1.30–1.09 (m, 12H) ppm; ^{13}C NMR (150 MHz, $CDCl_3$): δ 158.9, 158.4, 157.7, 151.9, 144.7, 139.3, 136.8, 136.7, 135.9, 135.9, 130.1, 130.0, 128.3, 128.2, 127.7, 127.6, 126.7, 126.7, 126.4, 125.7, 117.5, 116.3, 116.2, 113.0, 86.1, 86.1, 85.4, 85.4, 85.2, 84.0, 84.0, 73.1, 63.4, 63.1, 58.7, 58.5, 58.5, 58.4, 55.1, 45.4, 45.3, 43.3, 43.2, 41.3, 37.3, 37.0, 35.4, 24.7, 24.7, 24.6, 24.6, 24.5, 23.0, 22.9, 20.4, 20.4, 20.3, 20.2 ppm. ^{31}P NMR (81 MHz, $CDCl_3$): δ 149.4 and 149.2 ppm. MS ES+ *m/z*: 979 (MH^+); HR MALDI calcd for $C_{52}H_{59}F_3N_8O_6P$: 979.4242, found 979.4150.

Appendix A. Supplementary data

Supplementary data related to this article can be found at http://dx.doi.org/10.1016/j.ejmech.2014.03.081.

References

[1] K.K. Karlsen, A. Pasternak, T.B. Jensen, J. Wengel, Pyrene-modified unlocked nucleic acids: synthesis, thermodynamic studies, and fluorescent properties, ChemBioChem 13 (2012) 590–601.
[2] F. Hoevelmann, L. Bethge, O. Seitz, Single labeled DNA FIT probes for avoiding false-positive signaling in the detection of DNA/RNA in qPCR or cell media, ChemBioChem 13 (2012) 2072–2081.
[3] I.V. Astakhova, T.S. Kumar, J. Wengel, Fluorescent oligonucleotides containing a novel perylene 2′-amino-α-L-LNA monomer: synthesis and analytical potential, Collection of Czechoslovak Chemical Communications 76 (2011) 1347–1360.
[4] S. Latif, I. Bauer-Sardina, K. Ranade, K.J. Livak, P.-Y. Kwok, Fluorescence polarization in homogeneous nucleic acid analysis II: 5′-nuclease assay, Genome Research 11 (2001) 436–440.
[5] S.A.E. Marras, S. Tyagi, F.R. Kramer, Real-time assays with molecular beacons and other fluorescent nucleic acid hybridization probes, Clinica Chimica Acta 363 (2006) 48–60.
[6] D.W. Dodd, R.H.E. Hudson, Intrinsically fluorescent base-discriminating nucleoside analogs, Mini-Reviews in Organic Chemistry 6 (2009) 378–391.
[7] R.H.E. Hudson, A. Ghorbani-Choghamarani, Selective fluorometric detection of guanosine-containing sequences by 6-phenylpyrrolocytidine in DNA, Synlett 6 (2007) 870–873.
[8] M. Segal, B. Fischer, Analogues of uracil nucleosides with intrinsic fluorescence (NIF-analogues): synthesis and photophysical properties, Organic & Biomolecular Chemistry 10 (2012) 1571–1580.
[9] R.W. Sinkeldam, Y. Tor, New fluorescent nucleosides, Collection Symposium Series 12 (2011) 101–107.
[10] A.S. Wahba, M.J. Damha, R.H.E. Hudson, RNA containing pyrrolocytidine base analogs: increased binding affinity and fluorescence that responds to hybridization, Nucleic Acids Symposium Series 52 (2008) 399–400.
[11] L.M. Wilhelmsson, A. Holmen, P. Lincoln, P.E. Nielsen, B. Norden, A highly fluorescent DNA base analogue that forms Watson-Crick base pairs with guanine, Journal of the American Chemical Society 123 (2001) 2434–2435.
[12] L. Zilbershtein, A. Silberman, B. Fischer, 8-(p-CF3-cinnamyl)-modified purine nucleosides as promising fluorescent probes, Organic & Biomolecular Chemistry 9 (2011) 7763–7773.
[13] K. Evans, D. Xu, Y. Kim, T.M. Nordlund, 2-Aminopurine optical spectra: solvent, pentose ring, and DNA helix melting dependence, Journal of Fluorescence 2 (1992) 209–216.
[14] J. Smagowicz, K. Wierzchowski, Lowest excited states of 2-aminopurine, Journal of Luminescence 8 (1974) 210–232.

[15] M. Menger, T. Tuschl, F. Eckstein, D. Porschke, Mg2+-dependent conformational changes in the hammerhead ribozyme, Biochemistry 35 (1996) 14710–14716.
[16] J.T. Stivers, 2-Aminopurine fluorescence studies of base stacking interactions at abasic sites in DNA: metal-ion and base sequence effects, Nucleic Acids Research 26 (1998) 3837–3844.
[17] C.R. Guest, R.A. Hochstrasser, L.C. Sowers, D.P. Millar, Dynamics of mismatched base pairs in DNA, Biochemistry 30 (1991) 3271–3279.
[18] G. Kodali, K.A. Kistler, M. Narayanan, S. Matsika, R.J. Stanley, Change in electronic structure upon optical excitation of 8-vinyladenosine: an experimental and theoretical study, The Journal of Physical Chemistry A 114 (2010) 256–267.
[19] M. Daniels, W. Hauswirth, Fluorescence of the purine and pyrimidine bases of the nucleic acids in neutral aqueous solution at 300°K, Science 171 (1971) 675–677.
[20] N.B. Gaied, N. Glasser, N. Ramalanjaona, H. Beltz, P. Wolff, R. Marquet, A. Burger, Y. Mely, 8-vinyl-deoxyadenosine, an alternative fluorescent nucleoside analog to 2′-deoxyribosyl-2-aminopurine with improved properties, Nucleic Acids Research 33 (2005) 1031–1039.
[21] A.S. Wahba, A. Esmaeili, M.J. Damha, R.H.E. Hudson, A single-label phenylpyrrolocytidine provides a molecular beacon-like response reporting HIV-1 RT RNase H activity, Nucleic Acids Research 38 (2010) 1048–1056.
[22] C. Wanninger-Weiss, H.A. Wagenknecht, Synthesis of 5-(2-pyrenyl)-2′-deoxyuridine as a DNA modification for electron-transfer studies: the critical role of the position of the chromophore attachment, European Journal of Organic Chemistry 1 (2008) 64–71.
[23] M. Mizuta, K. Seio, A. Ohkubo, M. Sekine, Fluorescence properties of pyrimidopyrimidoindole nucleoside dCPPI incorporated into oligodeoxynucleotides, The Journal of Physical Chemistry B 113 (2009) 9562–9569.
[24] M. Mizuta, K. Seio, K. Miyata, M. Sekine, Fluorescent pyrimidopyrimidoindole nucleosides: control of photophysical characterizations by substituent effects, Journal of Organic Chemistry 72 (2007) 5046–5055.
[25] Z. Guo, X. Hao, F. Tan, X. Pei, L. Shang, X. Jiang, F. Yang, The elements of human cyclin D1 promoter and regulation involved, Clinical Epigenetics 2 (2011) 63–76.
[26] M. Wei, L. Zhu, Y. Li, W. Chen, B. Han, Z. Wang, J. He, H. Yao, Z. Yang, Q. Zhang, B. Liu, Q. Gu, Z. Zhu, K. Shen, Knocking down cyclin D1b inhibits breast cancer cell growth and suppresses tumor development in a breast cancer model, Cancer Science 102 (2011) 1537–1544.
[27] W.J. Kent, BLAT—the BLAST-like alignment tool, Genome Research 12 (2002) 656–664.
[28] M. Mizuta, K. Miyata, K. Seio, T. Santa, M. Sekine, Synthesis of fluorescent cyclic cytosine nucleosides and their fluorescent properties upon incorporation into oligonucleotides, Nucleic Acids Symposium Series 50 (2006) 19–20.
[29] M. Segal, E. Yavin, P. Kafri, Y. Shav-Tal, B. Fischer, Detection of mRNA of the cyclin D1 breast cancer marker by a novel duplex-DNA probe, Journal of Medicinal Chemistry 56 (2013) 4860–4869.
[30] P. Sandin, L.M. Wilhelmsson, P. Lincoln, V.E. Powers, T. Brown, B. Albinsson, Fluorescent properties of DNA base analogue tC upon incorporation into DNA—negligible influence of neighbouring bases on fluorescence quantum yield, Nucleic Acids Research 33 (2005) 5019–5025.
[31] C. Boiziau, B. Larrouy, B.S. Sproat, J.-J. Tolume, Antisense 2′-O-alkyl oligoribonucleotides are efficient inhibitors of reverse transcription, Nucleic Acids Research 23 (1995) 64–71.
[32] H. Inoue, Y. Hayase, A. Imura, S. Iwai, K. Miura, E. Ohtsuka, Synthesis and hybridization studies on two complementary nona(2′-O-methyl)ribonucleotides, Nucleic Acids Research 15 (1987) 6131–6148.
[33] S.M. Freier, K.-H. Altmann, The ups and downs of nucleic acid duplex stability: structure-stability studies on chemically-modified DNA: RNA duplexes, Nucleic Acids Research 25 (1997) 4429–4443.
[34] L. Clima, W. Bannwarth, Building-block approach for the straightforward incorporation of a new FRET (fluorescence-resonance-energy transfer) system into synthetic DNA, Helvetica Chimica Acta 91 (2008) 165–175.
[35] A.V. Tataurov, Y. You, R. Owczarzy, Predicting ultraviolet spectrum of single stranded and double stranded deoxyribonucleic acids, Biophysical Chemistry 133 (2008) 66–70.
[36] W. Melhuish, Quantum efficiencies of fluorescence of organic substances: effect of solvent and concentration of the fluorescent solute1, The Journal of Physical Chemistry 65 (1961) 229–235.
[37] P. Capek, R. Pohl, M. Hocek, Cross-coupling reactions of unprotected halopurine bases, nucleosides, nucleotides and nucleoside triphosphates with 4-boronophenylalanine in water. Synthesis of (purin-8-yl)- and (purin-6-yl) phenylalanines, Organic & Biomolecular Chemistry 4 (2006) 2278–2284.
[38] A. Collier, G.K. Wagner, Suzuki-Miyaura cross-coupling of unprotected halopurine nucleosides in water-influence of catalyst and cosolvent, Synthetic Communications 36 (2006) 3713–3721.
[39] D. Odadzic, J.B. Bramsen, R. Smicius, C. Bus, J. Kjems, J.W. Engels, Synthesis of 2′-O-modified adenosine building blocks and application for RNA interference, Bioorganic & Medicinal Chemistry 16 (2008) 518–529.